Preliminary study on the thorium-loaded accelerator-driven system with 100MeV protons at the Kyoto University Critical Assembly

AUTHOR(S):

Pyeon, Cheol Ho; Lim, Jae-Yong; Takemoto, Yuki; Yagi, Takahiro; Azuma, Tetsushi; Kim, Haksung; Takahashi, Yoshiyuki; Misawa, Tsuyoshi; Shiroya, Seiji

CITATION:

Pyeon, Cheol Ho ...[et al]. Preliminary study on the thorium-loaded accelerator-driven system with 100MeV protons at the Kyoto University Critical Assembly. Annals of Nuclear Energy 2011, 38(10): 2298-2302

ISSUE DATE:

2011-10

URL:

http://hdl.handle.net/2433/147269

Preliminary Study on the Thorium-Loaded Accelerator-Driven System with 100 MeV Protons at the Kyoto University Critical Assembly

Cheol Ho Pyeon[1,*], Jae-Yong Lim[1], Yuki Takemoto[2], Takahiro Yagi[2,**]

Tetsushi Azuma[2], Haksung Kim[2], Yoshiyuki Takahashi[2,**],

Tsuyoshi Misawa[1] and Seiji Shiroya[1,***]

[1]*Nuclear Engineering Science Division, Research Reactor Institute, Kyoto University, Asashiro-nishi, Kumatori-cho, Sennan-gun, Osaka 590-0494, Japan*

[2]*Department of Fundamental Energy Science, Graduate School of Energy Science, Kyoto University, Yoshida-honmachi, Sakyo-ku, Kyoto 606-8501, Japan*

(Received)

At the Kyoto University Critical Assembly (KUCA), spallation neutrons generated by high-energy proton beams are injected into the thorium-loaded systems on March 2010. By combining the Fixed Field Alternating Gradient (FFAG) accelerator with the thorium-loaded system at KUCA, a series of the ADS experiments is carried out under conditions whereby the spallation neutrons are generated at a tungsten target by 100 MeV protons at an intensity of 30 pA. Prompt neutron behavior in the time evolution is observed and thorium fission reactions are attained through the experiments and calculations, respectively. And the effects of neutron leakage and spectrum softening are experimentally observed through the neutron multiplication and reaction rate analyses. From the experimental and numerical analyses, in

* Corresponding author, Tel.: +81-72-451-2356; fax: +81-72-451-2603;
E-mail address: pyeon@rri.kyoto-u.ac.jp (C.H. Pyeon)
** Present address: Research Reactor Institute, Kyoto University,
Asashiro-nishi, Kumatori-cho, Sennan-gun, Osaka 590-0494, Japan
*** Present address: Nuclear Safety Commission of Japan,
3-1-1, Kasumigaseki, Chiyoda-ku, Tokyo 100-8970, Japan

the future, experimental conditions need to be improved to attain further neutron multiplication using the variation of fuels (thorium, highly-enriched and natural uranium) and moderators (graphite, polyethylene, aluminum and beryllium).

KEYWORDS: ADS, KUCA, FFAG accelerator, 100 MeV protons, tungsten target, proton beam injection, spallation neutrons, thorium fission reactions

1. Introduction

The concept of an energy amplifier with the accelerator-driven system (ADS) proposed in the 1990s (Carminati et al., 1993; Rubbia, 1995; Furukawa, 1997) was comprised of thorium (^{232}Th) fuel and a high-gain and -power accelerator. It was based on an essential feature (capture reactions) of ^{232}Th breeding into uranium-233 (^{233}U) as depicted below, whereas ^{232}Th demonstrated another important feature of a threshold reaction of approximately 2 MeV neutrons based on the fission ^{232}Th(n, f) shown in Table 1:

$$^{232}\mathrm{Th}\,(n,\gamma)\,^{233}\mathrm{Th}\xrightarrow[22.3\,\mathrm{m}]{\beta^-}\,^{233}\mathrm{Pa}\xrightarrow[26.967\,\mathrm{d}]{\beta^-}\,^{233}\mathrm{U}\quad .$$

The conversion ratio of capture and fission reactions was of interest mostly in the thorium fuel cycle through the development of several thorium-based reactors, including the molten-salt reactor, the high-temperature reactor, the light-water reactor and the heavy-water reactor. Subsequently, the feasibility of ADS based on the molten-salt reactor (comprising lead or lead-bismuth as coolant and ^{232}Th and ^{233}U fuel) was numerically investigated in the early 2000s (Bowman et al., 2000; Ishimoto et al., 2002; Vergnes et al., 2002), from the viewpoint of fuel recycling, as in the research and development of nuclear transmutation techniques.

At the Kyoto University Critical Assembly (KUCA), spallation neutrons generated by high-energy proton beams were successfully injected into thorium-loaded system on March 3rd, 2010, in addition to the first injection (Pyeon et al., 2009a) of high-energy proton beams in March 2009. By combining the Fixed Field Alternating Gradient (FFAG) accelerator (Tanigaki et al., 2010) with the thorium-loaded system at KUCA, a series of the ADS experiments was carried out under conditions whereby the spallation neutrons were generated at a tungsten target by 100 MeV protons at an intensity of 30 pA. The level of neutron yield

generated at the tungsten target was around 1×10^{7} 1/s. Regarding the two major reactions (capture and fission) of ^{232}Th, special attention was paid to the thorium fission reactions in the thorium-loaded ADS experiments. The objective of this study was to conduct preliminary study on the thorium-loaded ADS through the kinetic and static experiments using the high-energy neutrons: measurements of the subcriticality by the pulsed neutron method (Misawa et al., 2009) and the reaction rates for high-energy neutrons by the foil activation method, respectively.

2. ADS Experiments

2.1 Core configuration

The thorium-loaded systems (thorium; Fig. 1(a) and thorium-graphite; Fig. 1(b)) in the ADS experiments were composed of a 2”×2” square and 1/8” thick fuel plate (Fig. 2(a)), and 2”×2” square, and 1/8” and 1/2” thick fuel and graphite plates, respectively (Fig. 2(b)). By adding graphite to the thorium system, the effects of neutron leakage by a large size core and neutron spectrum softening by the graphite could be found in the thorium-graphite system. Then, the change in neutron multiplication caused by neutron leakage and spectrum softening was expected to be revealed in comparison with two thorium systems. As in the ADS experiments with 14 MeV neutrons at KUCA (Pyeon et al., 2009b, 2008, 2007; Taninaka et al., 2010), the target (tungsten) in thorium systems was located outside the core.

2.2 Kinetic experiments

For the evaluation of subcriticality by the pulsed neutron method with the use of prompt neutron decay measurements, neutron detectors (1/2”ϕ ^{3}He detectors; #1, #2, #3 and #4) were

set at four positions shown in Fig. 1: near the tungsten target (#1 at (18, A) and (19, A)); around the core (#2 at (15, H) and (15, J); #3 at (12, H) and (11, J); #4 at (12, D) and (11, E), Figs. 1(a) and 1(b), respectively). Resulting experimental data (#2, #3 and #4) were evaluated by considering the start time of measurement in neutron detector #1 at the target: the start time of measurement in other detectors #2, #3 and #4 was regarded as that in #1.

Prompt neutron behavior (Fig. 3) was experimentally attained by observing the time evolution of neutron density: an exponential-like decay revealed the time evolution of the decay behavior of high-energy neutrons in the thorium system, like the high-energy neutron transmission in the thorium system. And the change in thermal neutron density caused by the delayed neutrons was not observed in the region after the time evolution of about 1,000 μs. If the neutron decay behavior is caused by the scheme of delayed neutron generation after the fission by prompt neutrons, this behavior should have been experimentally observed in this system. However, as shown in Fig. 3, the decay behavior was considered to originate mainly from the high-energy neutrons in the entire time evolution, since an asymptotic behavior of delayed neutrons was not found for a long time evolution after 1,000 μs under the assumption that the delayed neutron components were independent of the time evolution. The reasons for this involved a small number of spallation neutrons (1×10^{7} 1/s) caused by a low intensity (30 pA) of protons, and a small number of fission neutrons by these spallation neutrons from the target.

In general, subcriticality can be deduced from the experimental results in prompt neutron decay constant used in the pulsed neutron method. Nonetheless, the asymptotic behavior by the delayed neutrons was not observed in the thorium system, as determined from the experimental results obtained at #2, #3 and #4, although the delayed neutron fraction of ^{232}Th (2.03%; fission by prompt neutrons) was large even by a comparison with that of ^{235}U (0.65%; fission by thermal neutrons). As a result, the subcriticality was not actually deduced in these kinetic experiments. On one hand, this fact was attributable to the same discussion on the delayed neutron components; on the other hand, to the results of the very small

multiplication: numerical values of the effective multiplication factor k_{eff}, obtained from MCNPX (Pelowitz, 2005) with the nuclear data library of ENDF/B-VII.0 (Chawick et al., 2006) (covering the cross-section of ^{232}Th for neutron energy up to 60 MeV), were 0.03250±0.00001 and 0.02399±0.00001 in the thorium and thorium-graphite systems, respectively. The eigenvalue calculations within a statistical error of less than 1% were executed using 2,000 active cycles of 100,000 histories.

2.3 Static experiments

High-energy neutron flux distribution was estimated by measurement of the ^{115}In(n, n')^{115m}In (threshold energy of 0.32 MeV neutrons) reaction rate distribution with the use of the foil activation method of indium foils (50×50×1 mm^3). The foils were set at an axial center position (beam injection position) of five fuel rods (15, A; B; D; E; G in Fig. 1) to obtain the information on high-energy neutrons in the systems. All foils were normalized by the ^{115}In(n, n')^{115m}In reactions excited in another indium foil (20×20×2 mm^3) setting at the tungsten target position to obtain the source neutron generation. In numerical analyses, the spallation neutrons were included in the MCNPX calculations by bombarding the tungsten target with 100 MeV protons. The indium foils were taken into account in the simulated calculations: the reaction rates were deduced from tallies taken in the indium foil setting regions. The results of source calculations by MCNPX with ENDF/B-VII.0 were obtained after 2,000 active cycles of 100,000 histories, which led to a statistical error of less than 1% in the reaction rates. The calculated reaction rate distributions (Fig. 4) agreed approximately with the experimental results and were within the statistical errors except at position (15, A) in both the thorium and thorium-graphite systems.

Nevertheless, the measured reaction rate distributions were included in the results in both source and thorium fission neutrons. Since the measured results in reaction rates of indium foils were not experimentally divided into source and thorium fission neutrons,

additional source calculations ("fission turnoff" option in MCNPX) of ^{232}Th were made to attain numerically the fission reactions of ^{232}Th themselves from the difference between fission and no-fission reactions: "fission turnoff" calculations were executed by taking the fission reactions with no-fission ones as follows:

$$RR_{total} = RR_{source} + RR_{fission} \quad , \tag{1}$$

$$RR'_{total} = RR_{source} \quad , \tag{2}$$

where RR_{total} indicates the calculated total reaction rates by MCNPX, including reaction rates RR_{source} and $RR_{fission}$ by source and fission neutrons, respectively. And, RR'_{total} indicates the calculated total reaction rates with "fission turnoff" option in MCNPX, such as reaction rate RR_{source} by source neutrons. Then, in Eq. (2), the neutron generation was assumed to be none after the reactions with high-energy neutrons and thorium. Finally, the difference between fission in Eq. (1) and no-fission in Eq. (2) was interpreted as the objective neutron generation from the thorium fuel in MCNPX calculations.

From the results in Fig. 4(a), the MCNPX calculations were considered reliable in the reaction rate analyses, comparing with the measured and calculated reaction rates in both thorium and thorium-graphite systems. On the basis of this calculation accuracy, the relative difference (Table 2) between RR_{total} and RR'_{total} in Eqs. (1) and (2), respectively, was clearly found to be about 25% at maximum in the calculated reaction rates: the thorium fission reactions were numerically attained from the relative difference shown in Table 2 and Fig. 4(b). In addition, the effect of neutron spectrum softening by graphite was comparable to the measured reaction rates (Table 3) of thorium and thorium-graphite systems. From the relative difference between measured reaction rates in two systems, the effect of neutron spectrum softening was clearly revealed over 50% at maximum in the core according to stepping away from the neutron source.

Meanwhile, a remarkable change in neutron multiplication by the neutron leakage and

spectrum softening was expected in the thorium-graphite system compared to the thorium system, however, the neutron multiplication was not obtained to be affected considerably by neutron leakage and spectrum softening in the thorium-graphite system, in comparison with the results in eigenvalue calculations described in Sec. 2.2. The reasons involved mainly the combination (ratio of fuel and moderator) and composition (fuel cell pattern) of thorium fuel and graphite. With regard to these analyses, the effects of neutron leakage and spectrum softening should contribute to making another core composed of other fuels (highly-enriched and natural uranium) and moderators (polyethylene, aluminum and beryllium) to attain more neutron multiplication than present core, leading to basic research on the next thorium-loaded ADS at KUCA.

3. Discussion

High-energy neutron spectra (Fig. 5) at the tungsten target position were observed not only in a static state but also by varying the time evolution for the injection of 100 MeV protons onto the target: the neutron flux was quickly attenuated in a very short time (a few μs at maximum). Moreover, the high-energy neutrons were considered to be dominant over around a few MeV energy at the tungsten target. Note that the MCNPX calculations with ENDF/B-VII.0 were executed by 2,000 active cycles of 100,000 histories in statistical error of less than 1%, and the neutrons were modeled by the injection of 100 MeV protons onto the tungsten. Besides the small number of spallation neutrons described in Sec. 2, another reason for the very small neutron multiplication (eigenvalues) in the thorium-loaded systems involved the behavior of neutron attenuation arisen at the tungsten target position shown in Fig. 5. This fact demonstrated that the high-energy neutrons were not sufficiently provided for the core to attain the neutron multiplication. Therefore, additional effort could be made to direct the highest number of high-energy neutrons generated by high-energy protons from

the FFAG accelerator to the core, like the neutron guide and beam duct (Pyeon, 2008) shown in the ADS experiments with 14 MeV neutrons at KUCA.

4. Concluding Remarks

Thorium-loaded ADS study was conducted as observed by the prompt neutron behavior and the reaction rates through the kinetic and static experiments, respectively. Actually, the thorium fission reactions were attained from the results in calculations of reaction rates, whereas subcriticality was not deduced from the results in measurements of neutron decay behavior, although the intensity and the neutron yield by 100 MeV protons were low in 30 pA and 1×10^{7} 1/s, respectively. In the future, while the proton beam commissioning is still under way to obtain the high intensity of protons, experimental conditions need to be improved to attain further neutron multiplication using the variation of fuels (thorium, highly-enriched and natural uranium) and moderators (graphite, polyethylene, aluminum and beryllium). Additionally, thorium capture reactions need to be elucidated, and the conversion ratio of capture and fission reactions needs to be examined experimentally in the thorium-loaded ADS at KUCA.

Acknowledgements

The authors are grateful to all the technical staff and the students of KUCA and the FFAG accelerator team for their generous assistance during the experiments.

References

Bowman, C.D., 2000. Once-through thermal-spectrum accelerator-driven light water reactor waster destruction without reprocessing. Nucl. Technol., 132, 66-93.

Carminati, F., Klapisch, R., Revol, J.P., et al., 1993. An energy amplifier for cleaner and inexhaustible nuclear energy production driven by a particle beam accelerator. CERN/AT/93-47.

Chadwick, M.B., Obložinský, P., Herman, M., et al., 2006. ENDF/B-VII.0: Next generation evaluated nuclear data library for nuclear science and technology. Nucl. Data Sheets, 107, 2931-3060.

Furukawa, K., 1997. Thorium cycle implementation through plutonium incineration by thorium molten-salt nuclear energy synergetics. IAEA-TECDOC-1319.

Ishimoto, S., Ishibashi, K., Tenzou, H., et al., 2002. Neutronics study on accelerator driven subcritical systems with thorium-based fuel for comparison between and molten-salt fuels. Nucl. Technol., 138, 300-312.

Misawa, T., Unesaki, H, Pyeon, C.H., 2010. Nuclear Reactor Physics Experiments, Kyoto University Press, Kyoto, Japan, pp.119-129.

Pelowitz, D.B., 2005. MCNPX User's Manual, Version 2.5.0.," LA-CP-05-0369, Los Alamos National Laboratory.

Pyeon, C.H., Misawa, T., Lim, J.Y., et al., 2009a. First injection of spallation neutrons generated by high-energy protons into the Kyoto University Critical Assembly. J. Nucl. Sci. Technol., 46, 1091-1093.

Pyeon, C.H., Shiga, H., Misawa, T., et al., 2009b. Reaction rate analyses for an accelerator-driven system with 14 MeV neutrons in the Kyoto University Critical Assembly. J. Nucl. Sci. Technol., 46, 965-972.

Pyeon, C.H., Hervault, M., Misawa, T., et al., 2008. Static and kinetic experiments on accelerator-driven system with 14 MeV neutrons in Kyoto University Critical Assembly. J. Nucl. Sci. Technol., 45, 1171-1182.

Pyeon, C.H., Hirano, Y., Misawa, T., et al., 2007. Preliminary experiments on

accelerator-driven subcritical reactor with pulsed neutron generator in Kyoto University Critical Assembly. J. Nucl. Sci. Technol., 44, 1368-1378.

Rubbia, C., 1995. A high gain energy amplifier operated with fast neutrons. In: AIP Conference Proceedings, 346, 44-53; see also 1994. In: Proceedings of International Conference on Accelerator-Driven Transmutation Technologies and Application, Las Vegas, July 25-29.

Tanigaki, M., Takamiya, K., Yoshino, H., et al., 2010. Control system for the FFAG complex at KURRI. Nucl. Instrum. Methods A, 612, 354-359.

Taninaka, H., Hashimoto, K., Pyeon, C.H., et al., 2010. Determination of lambda-mode eigenvalue separation of a thermal accelerator-driven system from pulsed neutron experiment. J. Nucl. Sci. Technol., 47, 376-383.

Vergnes, J., Lecarpentier, D., 2002. The AMSTER concept (actinide molten salt transmutER). Nucl. Eng. Des., 216, 43-67.

Figure captions

Fig. 1(a) Top view of the configuration of thorium system

Fig. 1(b) Top view of the configuration of thorium-graphite system

Fig. 2(a) Side view of the configuration of fuel rod for “Th” shown in Fig. 1(a)

Fig. 2(b) Side view of the configuration of fuel rod for “TG” shown in Fig. 1(b)

Fig. 3 Experimental results in neutron decay behavior at three positions in the thorium system

Fig. 4(a) Comparison between measured and calculated reaction rate distributions at positions (15, A; B; D; E; G) in Fig. 1

Fig. 4(b) Comparison between calculated reaction rate distributions at positions (15, A; B; D; E; G) in Fig. 1 of the thorium system

Fig. 5 Neutron spectra in the static and the time evolution for the injection of 100 MeV protons onto the tungsten target

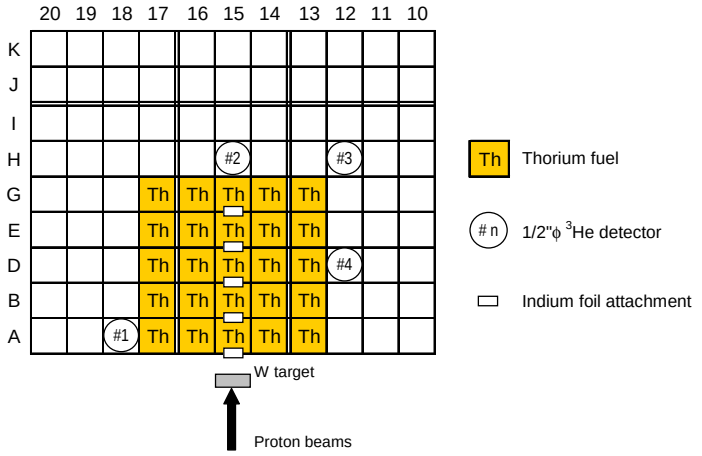

Fig. 1(a) Top view of the configuration of thorium system

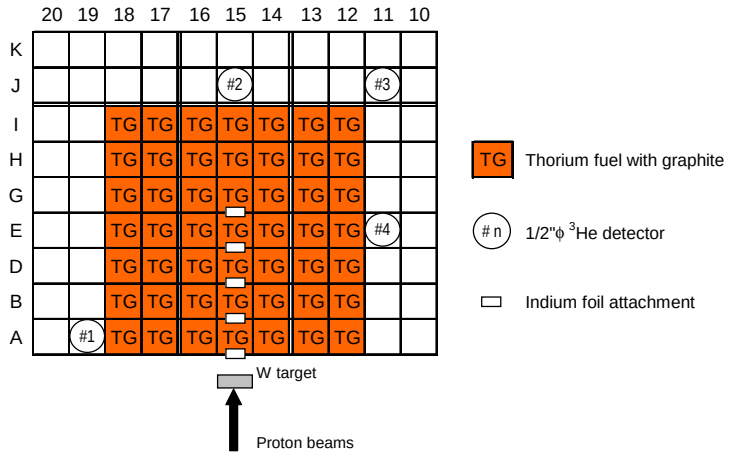

Fig. 1(b) Top view of the configuration of thorium-graphite system

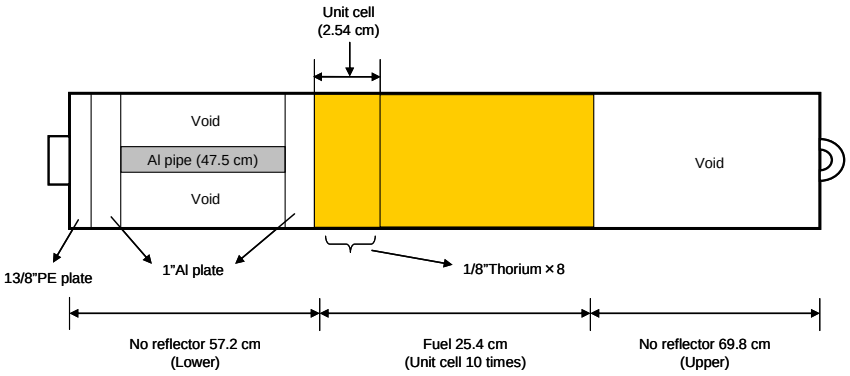

Fig. 2(a) Side view of the configuration of fuel rod for “Th” shown in Fig. 1(a)

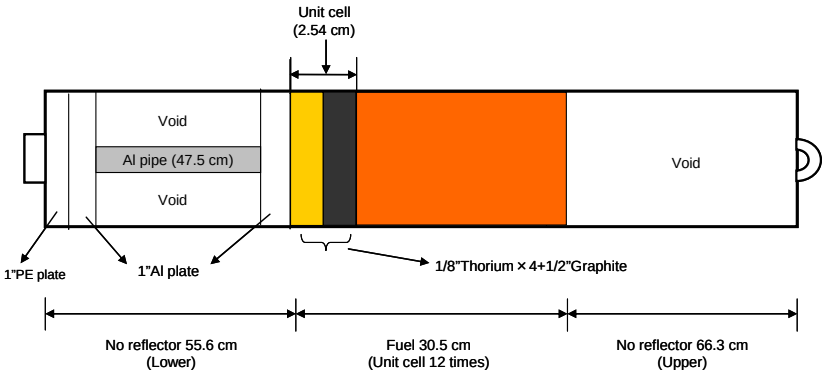

Fig. 2(b) Side view of the configuration of fuel rod for “TG” shown in Fig. 1(b)

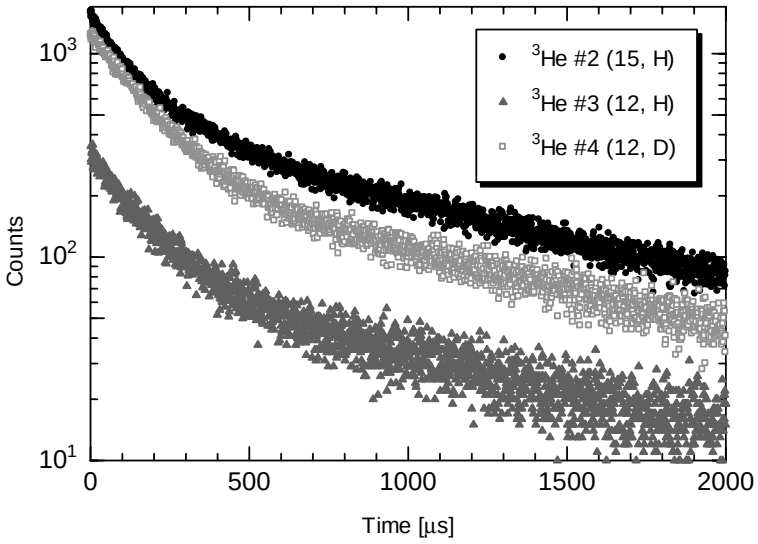

Fig. 3 Experimental results in neutron decay behavior at three positions in the thorium system

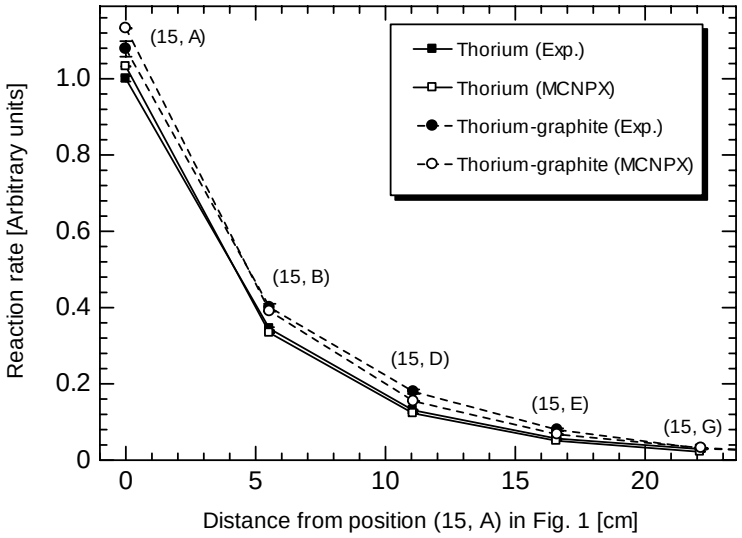

Fig. 4(a) Comparison between measured and calculated reaction rate distributions at positions (15, A; B; D; E; G) in Fig. 1

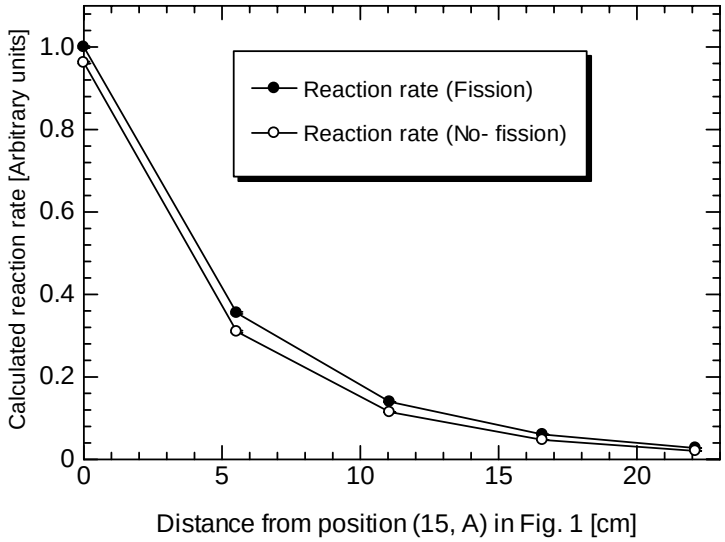

Fig. 4(b) Comparison between calculated reaction rate distributions at positions (15, A; B; D; E; G) in Fig. 1 of the thorium system

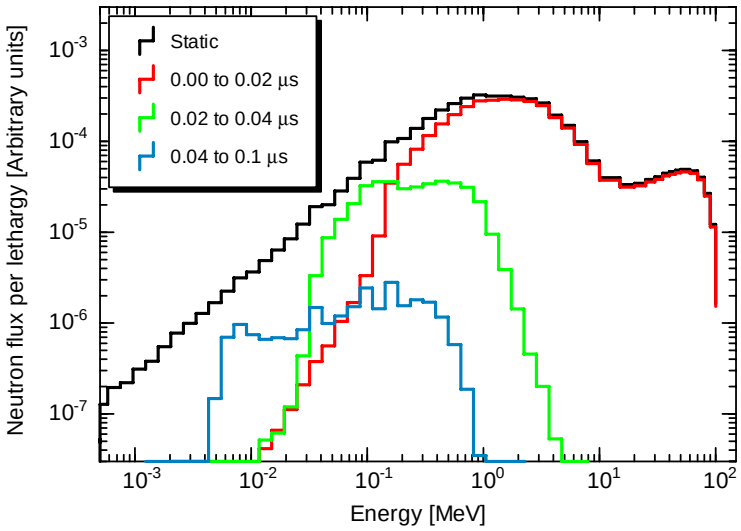

Fig. 5 Neutron spectra in the static and time evolution for the injection of 100 MeV protons onto the tungsten target

Table captions

Table 1 Main characteristics of nuclides obtained by thorium fission reactions

Table 2 Comparison between calculated reaction rates in the thorium system

Table 3 Comparison between measured reaction rates in the thorium and thorium-graphite

Table 1 Main characteristics of nuclides obtained by thorium fission reactions

Nuclide	Half-life	γ-ray energy [keV]	Emission rate [%]	Yield of fission products [%]
^{91}Sr	9.48 h	1024.3	34.01	7.36
^{92}Sr	2.71 h	1383.9	90.00	6.92
^{97}Zr	17 h	743.4	94.60	4.43
^{135}I	6.7 h	1260.5	30.28	5.52
^{142}La	1.55 h	641.2	48.90	6.52

Table 2 Comparison between calculated reaction rates in the thorium system

Distance [cm] (Position)	Reaction rate [1/cm^3/source]		Relative difference [%]
	RR_{total} in Eq. (1)	RR'_{total} in Eq. (2)	
0.00 (15, A)	$(3.97\pm0.01)\times10^{-6}$	$(3.82\pm0.01)\times10^{-6}$	3.8
5.53 (15, B)	$(1.40\pm0.01)\times10^{-6}$	$(1.23\pm0.01)\times10^{-6}$	12.1
11.06 (15, D)	$(5.54\pm0.01)\times10^{-7}$	$(4.55\pm0.01)\times10^{-7}$	17.9
16.59 (15, E)	$(2.40\pm0.01)\times10^{-7}$	$(1.87\pm0.01)\times10^{-7}$	22.1
22.21 (15, G)	$(1.09\pm0.01)\times10^{-7}$	$(8.13\pm0.04)\times10^{-8}$	25.4

Table 3 Comparison between measured reaction rates in the thorium and thorium-graphite systems

Distance [cm] (Position)	Reaction rate [1 /cm^3/s]		Relative difference [%]
	Thorium system	Thorium-graphite system	
0.00 (15, A)	$(5.32\pm0.07)\times10^{-2}$	$(6.06\pm0.13)\times10^{-2}$	13.9
5.53 (15, B)	$(1.92\pm0.03)\times10^{-2}$	$(2.16\pm0.06)\times10^{-2}$	12.5
11.06 (15, D)	$(7.39\pm0.15)\times10^{-3}$	$(8.51\pm0.32)\times10^{-3}$	15.2
16.59 (15, E)	$(3.15\pm0.08)\times10^{-3}$	$(4.38\pm0.21)\times10^{-3}$	39.0
22.21 (15, G)	$(1.39\pm0.04)\times10^{-3}$	$(2.17\pm0.13)\times10^{-3}$	56.1